PHOTOCATALYTIC DEGRADATION OF REACTIVE YELLOW 23 IN AQUEOUS SOLUTIONS CONTAINING TiO$_2$ SUSPENSIONS

Imen BOUZAIDA [a,b], Corinne FERRONATO [a], Jean Marc CHOVELON [a],
Mohamed El Baker RAMMAH [b*], Jean Marie HERRMANN [a]

[a] *laboratoire d'application de la chimie à l'environnement (LACE), UMR-CNRS 5634,*
Université Claude Bernard Lyon 1,43 Bd du 11 novembre 1918, 69622 Villeurbanne Cedex, France
[b] *laboratoire de chimie organique hétérocyclique-LCOH/LCOHSNR-LR11ES39, Département de Chimie,*
Faculté des Sciences, Université de Monastir, 5019 Monastir, Tunisie

Abstract: The photocatalytic degradation of the mono azo dye Reactive Yellow 23 was investigated in aqueous solutions containing TiO$_2$ suspension as photocatalyst . Results showed that adsorption played an important role in the photocatalytic degradation rate. By comparing the disappearance of RY23 followed by HPLC-DAD (high performance liquid chromatography-diode array detector) and the bleaching of the solution followed by UV-Vis spectrometry (wavelength of analysis = 430 nm), two different kinetics were found proving that some of the intermediate products were still colored. This was confirmed using HPLC-DAD and HPLC-MS (high performance liquid chromatography- mass spectrometry) analysis. The degradation of RY23 should lead to the formation of carboxylic acids (formic, acetic and oxalic). The decrease of Total Organic Carbon (TOC) in dye solution was measured to monitor the dye mineralization process. Major identified intermediates are hydroxylated derivatives. The Langmuir kinetic treatment was chosen because it has already been successfully used to describe solid-liquid reactions of photocatalytic degradation.

Introduction

Dyestuff and dyeing industry have long been important textile industries in Tunisia. However, about 1-20% of dyes is lost during the dyeing process and is released in the textile effluents [1-5]. As a result, the effluents that are characterized with high color, low biodegradability and high variability have seriously polluted the drain water. Heterogeneous photocatalysis appears as an emerging and interesting technology for the degradation of organic pollutants such as dyes as it can utilize sunlight as source of energy, which is free and inexhaustible [6-13]. Unfortunately, only 5% of the solar energy reaching the earth's surface can be absorbed by a classical photocatalysts such as titania. For practical application of dye wastewater treatment by TiO2- UV process, there is a need to determine the optimal conditions of experimental parameters for economic removal of the dye. Of the dyes available on the market today, approximately 50-70% are azo compounds followed by the anthraquinone group. Azo dyes can be divided into monoazo, diazo triazo classes according to the presence of one or more azo bonds (-N=N-) and found in various categories, acid, basic, direct, disperse, azoic and pigments [3,5,14]. Therefore azo dyes are polluants of high environmental impact and were selected as the most relevant group of dyes concerning their degradation using TiO2 assisted photocatalysis.

In the present investigation, a reactive class monoazo dye, Reactive Yellow 23, has been chosen to evaluate its removal by photocatalytic treatment. A special attention has been paid to the identification of intermediates.

[*] Corresponding author, e-mail : mohamedelbaker.rammah@fsm.rnu.tn

2. Material and procedure

2.1. Materials and reagents

Reactive Yellow 23 = $C_{19}H_{14}N_5O_{13}S_3Na_3$ (dye content 90 %, the 10 % remaining products do not absorb in the spectral range 200-900 nm) was purchased from Hoechst and is extensively used in dyeing the textile fabrics. The chemical structure was given in igure 1 and its elemental analysis given in table I. Methanol for HPLC analysis was obtained from Fisher Chemical (Loughborough. Leics. UK). Deionised water was produced by a Milli-Q system and used systematically. The photocatalyst was TiO_2 Degussa P-25, mainly anatase (80%), with a specific surface area of 50 $m^2.g^{-1}$ and a mean particle size of 30 nm.
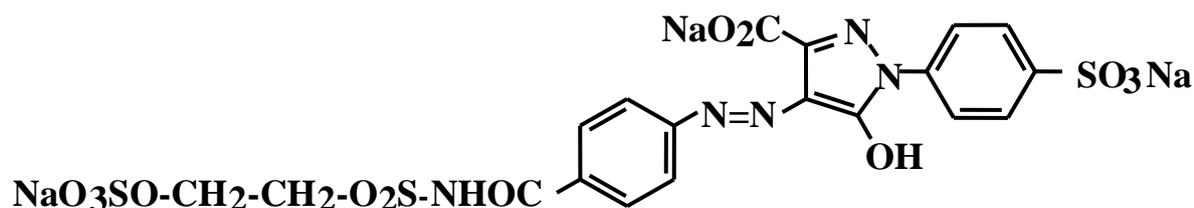
Table I Elemental analysis of Reactive Yellow 23

	% C	% N	% H	% S	% Na	% Cl
Reactive Yellow 23	28.46	6.59	2.66	12.07	13.52	0.45

2.2. Photoreactor and light source

The irradiation experiments were carried out in a 60 mL Pyrex cylindrical flask, open to air, with an optical window (at the bottom) of about 3 cm in diameter and a thermostated water-circulating jacket of about 6 cm diameter. It was mounted at a distance of 6 cm from the top of the lamp assembly, which consisted of a horizontal Philips HPK 125 W mean pressure mercury lamp. The light intensity could be reduced by intercaling metallic calibrated grids between the lamp and the reactor. The light intensity received by the solutions was evaluated using uranyle oxalate as actinometer. It was found that the number of the photons potentially absorbable by TiO_2 in the irradiation cell could at 4×10^{15} photons per second. For all experiments, the suspensions were magnetically stirred.

2.3. Procedure

A volume of 25 ml of aqueous solution of RY23 was introduced in the reactor. Adsorption and degradation were carried out at 20°C. The pH was adjusted either by using NaOH or HNO_3. To determine the adsorption constants, different concentrations of RY23 were used. Before analysis, aliquots of the aqueous suspensions were collected at selected time intervals and filtered through 0.45 PVDF filters (Millipore) to remove TiO_2 particles.

2.4. Analyses

The UV-Vis absorption spectra were recorded using a double-beam UVIKON spectrophotometer (Kontron Instruments)

The HPLC –DAD analyses were performed using a Shimadzu HPLC system. The column was a HYPERSIL BDS C_{18}. 5µm. (125 x 4 mm), the flow rate was 1mL.min⁻¹ and the injection volume was 20 µL. The mobile phase was methanol (A) and water + 0.03 $mol.L^{-1}$ of ammonium acetate (B). The isocratic elution conditions were 37 % (A) + 63 % (B) and the retention time was 9.1 min for RY23. The wavelength for detection was 430 nm which was chosen at the maximal absorption value for RY23. Total Organic Carbon (TOC) was determined using a Shimadzu TOC analyser (model 5050 A). The HPLC-MS identification of photoproducts was performed using a Hewlet-Packard HP 1100 series LC-MSD. The column was a Uptishere C18 HDO 3

μm (150 x 3 mm) and the mobile phase was methanol (A) and water + 0.03 mol.L^{-1} of ammonium acetate (B). A gradient elution was used from 0 to 100% (A) in 20 min. The MS detection was performed with electrospray ionisation (ESI) in negative and positive modes.

3. Results and Discussion
### 3.1. Preliminary adsorption in the dark :
Adsorption of pollutants on the semiconductor surface is an important parameter in heterogeneous photocatalysis. The adsorption experiments have been carried out in order to evaluate the equilibrium constants of adsorption. First of all, different concentrations of RY23 were used to study their adsorption isotherm (T = 20°C and pH 7.2). Whatever the initial concentrations (from 13 μmol.L^{-1} to 92 μmol.L^{-1}), it was found that an equilibrium adsorption of a Langmuirian type was reached in less than 25 minutes. The Langmuir kinetic treatment was chosen because it have already been successfully used to describe solid-liquid reactions of photocatalytic degradation as has been studied for a later publication [15,16].
 According to the Langmuir model the coverage θ varies as

$$\theta = Q_{ads} / Q_{max} = KC_{eq}/(1 + KC_{eq}) \tag{1}$$

where Q_{ads} is the number of adsorbed molecules at the adsorption equilibrium, Q_{max} the maximal adsorbable quantity, K the Langmuir adsorption constant of RY23 on TiO_2 and C_{eq} the concentration of RY23 at the adsorption equilibrium.
Figure 2 shows that the quantity adsorbed (Q_{ads}) increases with concentration at the adsorption equilibrium (C_{eq}). This behavior looks like the classical Langmuir adsorption model.
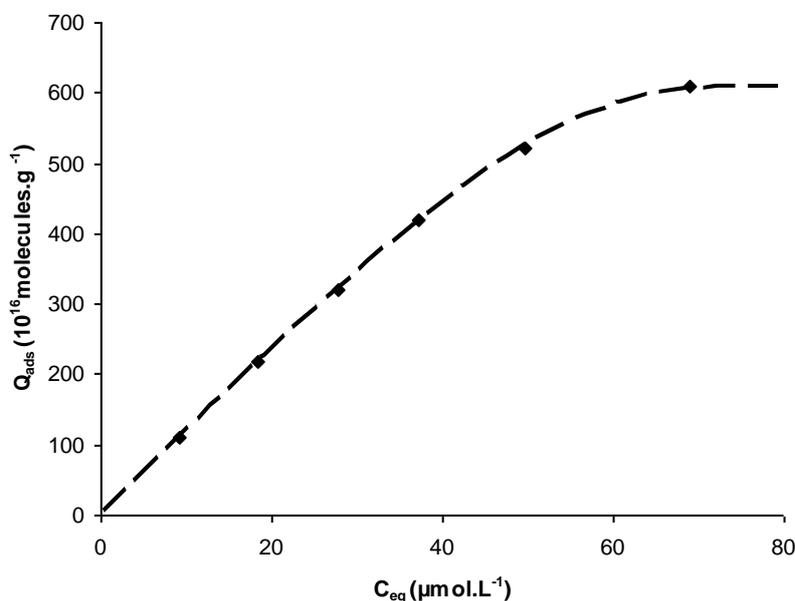

Figure.2 Langmuir adsorption isotherm of RY23 on TiO2: quantities adsorbed as function of equilibrium concentration.

Figure 3 represents the linear transformation of Eq (1) which is expressed by the following equation

$$1/Q_{ads} = 1/ Q_{max} + 1/ (Q_{max} K C_{eq}) \tag{2}$$

In this curve, the ordinate at the origin is equal to the reciprocal of Q_{max}, whereas K can be calculated from the slope (slope = 1/ Q_{max} K).
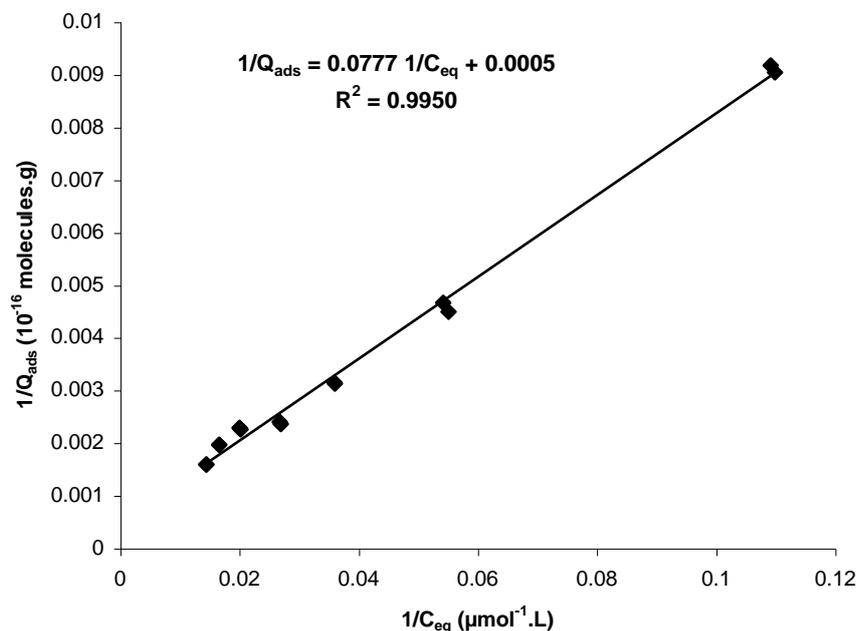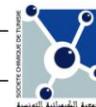
Figure.3 Transformation of Langmuir isotherm: reciprocal of the quantity adsorbed as a function of reciprocal of equilibrium concentration (pH 7.2 and T= 20°C).

In table II, adsorption parameters (Q_{max} and K) for RY23 were reported, as well as the maximal coverage of TiO_2 determined by taking into account the maximum number of adsorption sites estimated to be equal to 5 mol nm^{-2}. It appears that the value of K is in agreement with that of other dyes which have an analogous structure [5,17-24] . For example for orange G which is also a monoazo dye, a value of 5640 L.mol^{-1} has been found [24] against a present value of 6435 L.mol^{-1}. Anyway, such a value has to be used carefully since a very slight variation in the calculation of the slope can give rise to a significant variation of K values.

Table II Adsorption parameters (Q_{max} and K) for RY23

	K_{ads} (L.mol^{-1})	Q_{max} (µmol.g^{-1})	Q_{max} (molecules.nm^{-2})	θ_{max} (%)
RY23	**6435**	**33.2**	**0.4**	**8**

3.2. Photocatalytic degradation of RY23

For the subsequent experiments, the dye solution was magnetically stirred in the dark during 30 min before irradiating the reactor to make sure that adsorption equilibrium was reached. During c intermediates are formed and may interfere in the determination of kinetics because of competitive adsorption and degradation. Therefore calculations were done for conversions smaller than 15%. During this interval of time, the influence of intermediates could be considered as negligible.

3.2.1. Kinetic studies

Figure 4, shows the changes in the RY23 optical densities as a function of different time irradiation. The spectra present two main maxima, one at 430 nm and the other one at 250 nm, the one at 430 nm being responsible of the colour of the dye. The complete decolourisation is achieved at 180 min of irradiation time but degradation of intermediates continues up to 240 mn. The fast decolourisation of dye is due to the initial electrophilic cleavage of its chromophoric azo (-N=N-)

bonds. The degradation of aromatic part of the dye molecule produced number of intermediate compounds and the removal of these intermediates took longer time.
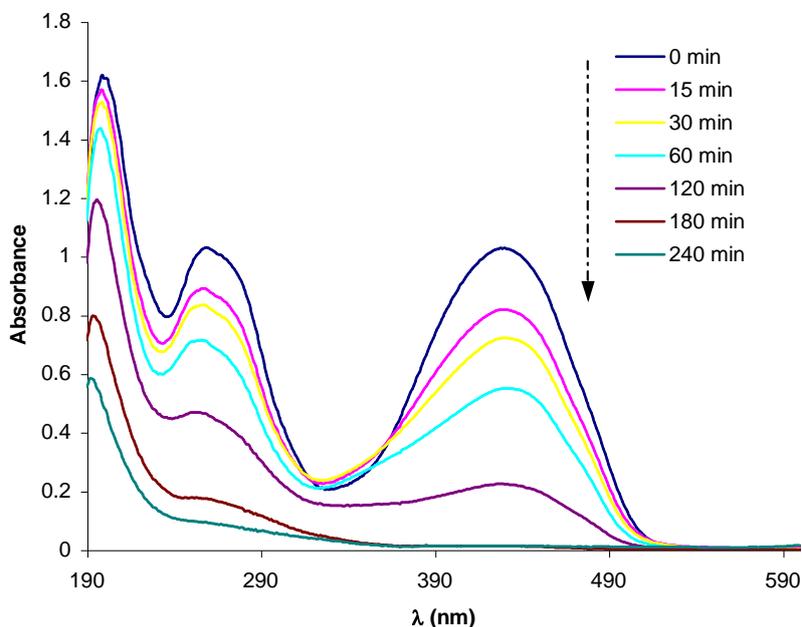
**Figure.4** UV- Vis spectra of RY23 as a function of irradiation time.
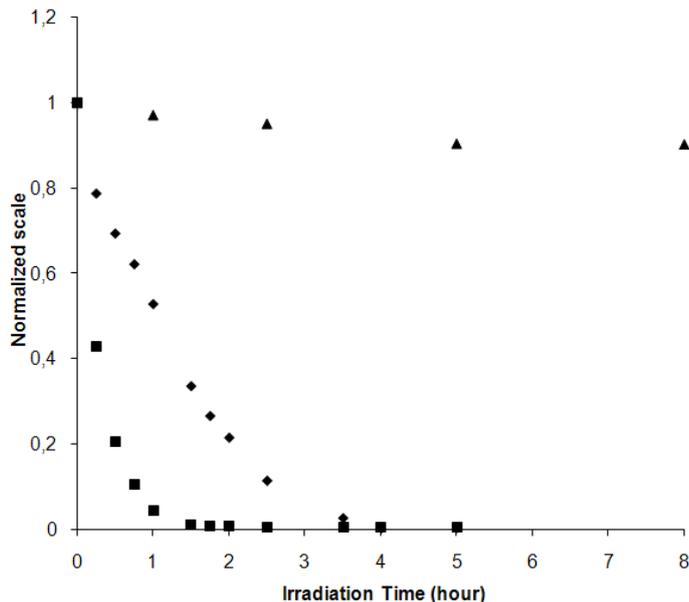

Figure.5 Photocatalytic degradation of RY23 followed by HPLC-DAD (■) and followed by UV-Vis spectrometry (♦). For both experiments a wavelength of analysis of 430 nm was chosen. Photolytic degradation of RY23 followed by HPLC-DAD (▲). For all experiments, the photon flux measured by actinometry was $0.4.10^{16}$ photon.s^{-1}.

Figure 5 shows both disappearance of RY23 and bleaching of the solution followed by HPLC-DAD and UV-Vis spectrometry, respectively (wavelength of analysis = 430 nm). Information obtained from both curves are different but complementary, since HPLC measures only RY23 disappearance, whereas spectrometry follows all the products absorbing at 430 nm (RY23 plus intermediates). From these curves, the half-reaction times calculated by assuming an apparent first-order kinetic law as it will presented in the next section, are 8 minutes ($k = 9.44 \times 10^{-2}$ min^{-1}) and 66 minutes ($k = 1.06 \times 10^{-2}$ min^{-1}) for disappearance of RY23 and for bleaching, respectively. As these results are not equivalent, we can conclude that some of the intermediate products were still colored. This was confirmed (i) by the photoproducts UV spectra (from HPLC-DAD) and (ii) by HPLC-MS analysis which allow us to tentatively identify the main photoproducts (cf. Table 3).

Table III shows that almost all photoproducts observed after 30 min of degradation still maintain a monoazo structure (except intermediates 3 and 5), some of them resulting from a direct hydroxylation of the initial molecule.

Table III : photoproducts observed after 30 min of degradation

| Photoproducts	Mass ES⁻: electrospray negatif ES⁺: electrospray positif
(**RY23**) NaO_2C ... SO_3Na $NaO_3SO - C_2H_4 - O_2S - NHOC$ ... $N=N$ ... OH	$M = 685$ g.mol^{-1} $t_r = 40.9$ min ES⁻ : 596 [M – COONa – Na⁺ + H⁺]⁻ ES⁺: 598 [MH – COONa – Na⁺ + 2H⁺]⁺
Product 1 HO_2C ... OH ... OH $HO_3SO - C_2H_4 - O_2S - NHOC$ ... $N=N$ ... OH ... OH	$M = 587$ g.mol^{-1} $t_r = 24.4$ min ES⁻ : 586 [M-H⁺]⁻
Product 2 H ... N ... SO_3Na $N=N$ ... OH	$M = 366$ g.mol^{-1} $t_r = 26.1$ min ES⁻ : 343 [M-Na⁺]⁻
Product 3 HO_2C ... N ... SO_3Na H_2N ... OH	$M = 343$ g.mol^{-1} $t_r = 27.6$ min ES⁻ : 320 [M-Na⁺]⁻
Product 4 HO_2C ... N ... OH $N=N$ ... OH $HO_3SO - C_2H_4 - O_2S - NHOC$ ... OH	$M = 571$ g.mol^{-1} $t_r = 28.1$ min ES⁻ : 570 [M-H⁺]⁻
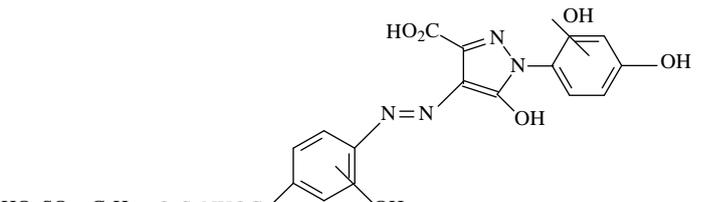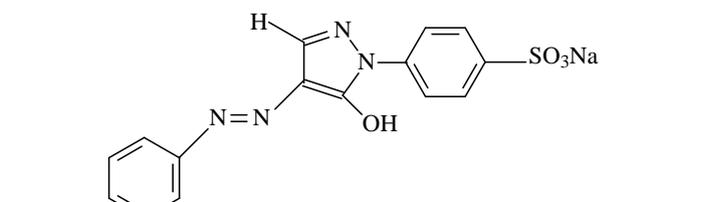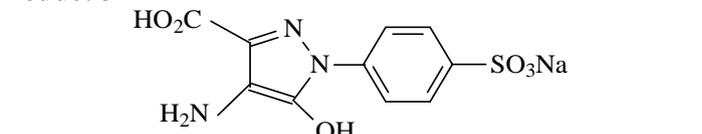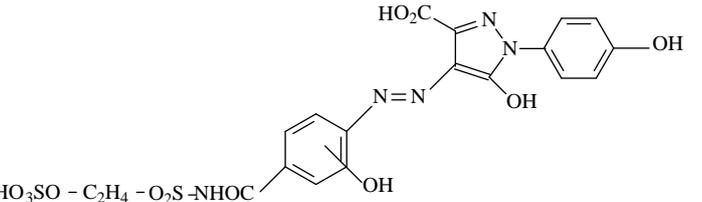
Photoproducts	Mass ES⁻: electrospray negatif ES⁺: electrospray positif
Product 5	$M = 325$ g.mol^{-1} $t_r = 33.6$ min ES$^+$: 326 [MH+ H$^+$] $^+$
Product 6	$M = 613$ g.mol^{-1} $t_r = 38.0$ min ES$^-$: 612 [M-H$^+$] $^-$ ES$^+$: 614 [MH+H$^+$] $^+$
Product 7	$M = 362$ g.mol^{-1} $t_r = 42.9$ min ES$^-$: 361[M-H$^+$] $^-$ 345 [M- OH$^-$] $^-$
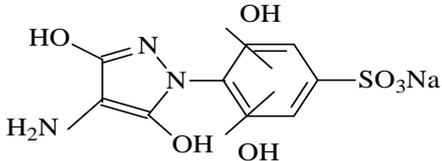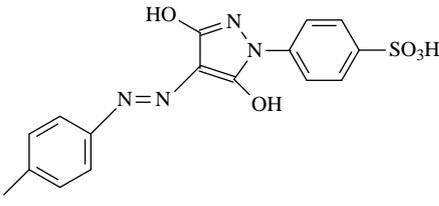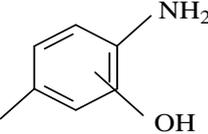
Figure 5 also shows disappearance of RY23 without TiO$_2$ to compare the efficiency of the photocatalytic degradation with that of direct photolysis. As expected, the direct photolysis is much slower than photocatalytic degradation since a half-time of 36 hours (k = 1.93 x 10^{-2} h^{-1}) was obtained. This means that photocatalytic degradation is not in concurrence with direct photolysis.

Figures 6 and 7, represent the evolution of intermediate products identified during the photocatalytic degradation of RY23. Almost all the photoproducts contain at least one hydroxyl group which was added on the aromatic cycle during the degradation.
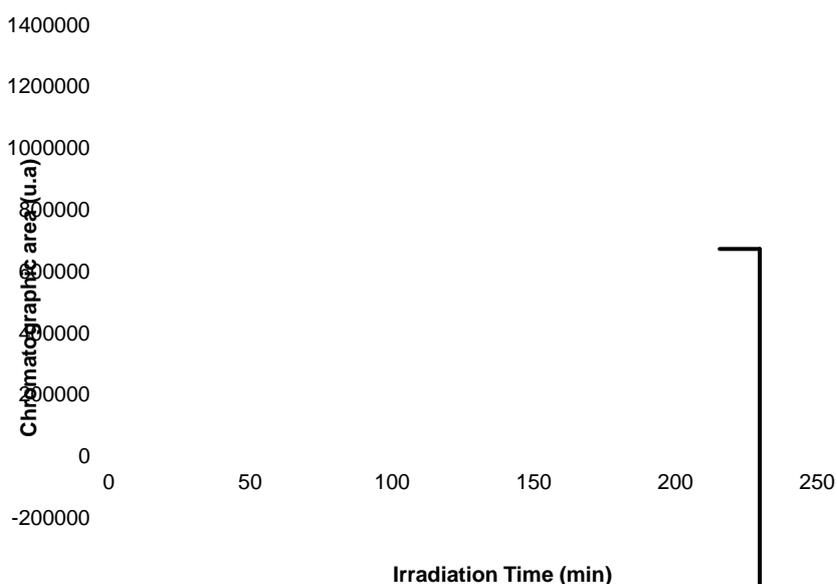

Figure.6 Evolution of the photoproducts detected during RY23 photocatalytic degradation (photonic flux: 0.4 10^{16} photons per second). The identities of products are given in table 3.

Thus, one can note one intermediate which is formed in relatively large quantity if it is considered that its absorption coefficient is not very different from that of the RY23 (the same chromophore) contain two hydroxyl groups added on RY23 (Figure 6)

By looking Figure 7, we can notice that at 180 minutes of irradiation almost all the molecule containing a chromophore have disappeared, which is in agreement with figure 4.

We can suppose that intermediate 3 which lost the azo structure is the main responsible of the decolorization of the effluent taking into account its relative abundance.
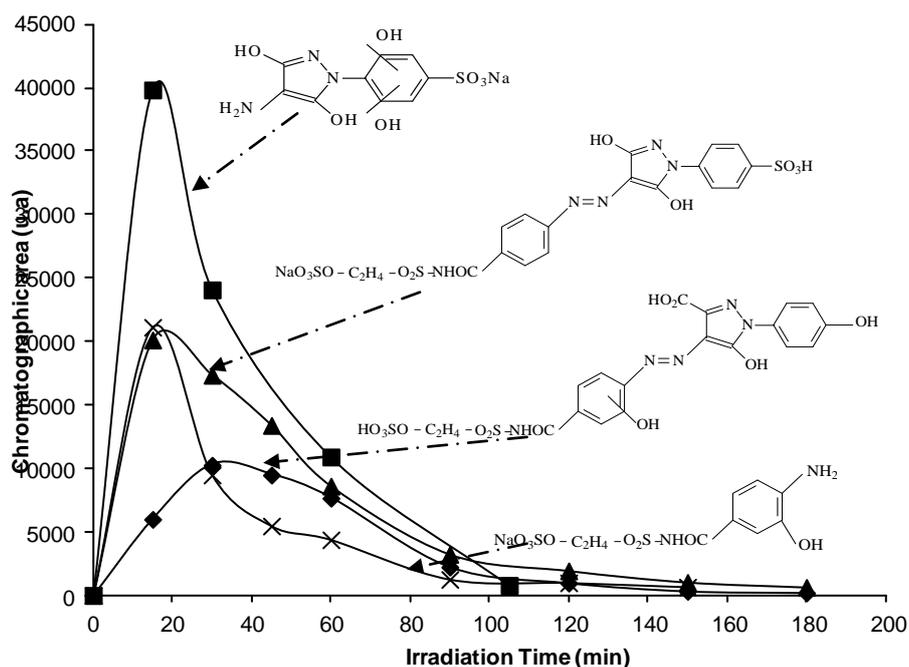
Figure.7 Evolution of the photoproducts detected during RY23 photocatalytic degradation (photonic flux: 0.4 10^16 photons per second). The identities of products are given in table 3.

According to the intermediates identified in table 3, 4 main reactions of degradation can be proposed. Reaction of hydroxylation and of desulfonation (product 1, product 4, product 5 and product 7), Photo_kolbe reaction (product 6) and the rupture of N=N (product 5).

Figure 8 presents the mineralization kinetic followed by TOC measurements. We can notice that the mineralization is not total. Indeed, after 64 hours of irradiation only 80 % of the quantity of initial organic carbon in the molecule of RY23 were transformed into CO_2. This might be explained by:

- A problem of calibration.
- The impurity of dye (pure 90 %).
- The low degradability of a part of the molecule.

We can exclude the problem of the calibration because several blanks have been done. In this context we can propose that molecule presented in Figure 9 which is known to be very stable could be responsible of the remaining 20% of the initial quantity of carbon in the molecule. This molecule contains 3 carbon atoms which represent 16 % of a number of carbon in the molecule, not far from the 20%.
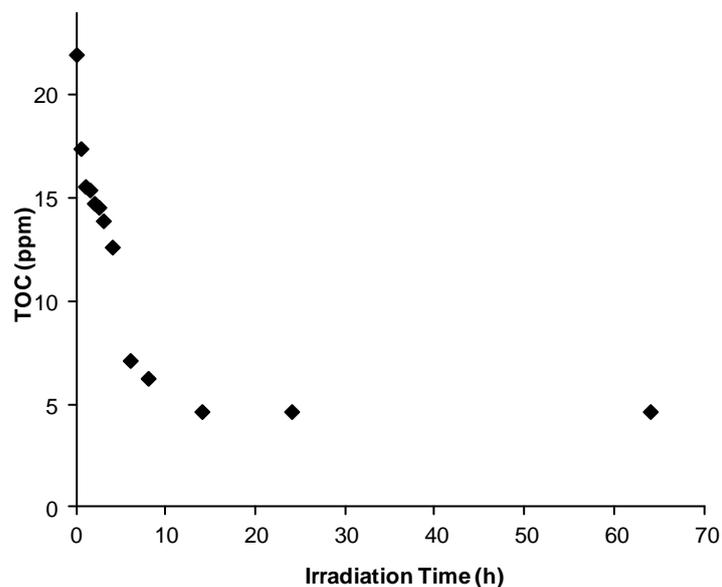
Figure.8 Photocatalytic degradation of RY23 followed by TOC analysis.
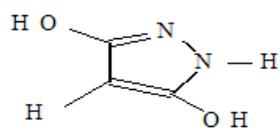
Figure.9 Molecul proposed

3.2.2. Carboxylic acids evolution:
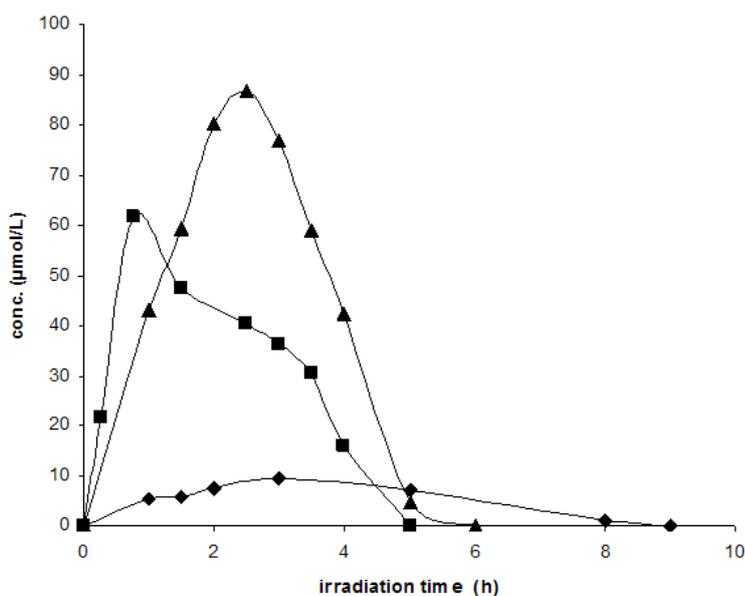
Figure.10 Formation of carboxylic acids (photonic flux: 0.4 10[16] photons per second) (■formic, ◆oxalic, ▲acetic)

The degradation of RY23 should lead to the formation of smaller and more oxidized intermediates, such as short carboxylic acids (formic, acetic and oxalic). Their evolution has been followed using HPLC-DAD. Acetic acid is rapidly formed, its concentration increases for about 150 min and rapidly disappears. The formation of acetic acid can be attributed to the aromatic ring opening [25].

Formic acid also rapidly appeared, reaching its maximum concentration at 45 min and then rapidly disappears.

Oxalic acid is formed to a long extent, reaching the maximum concentration at 180 min and disappears after 9 hours Figure 10.
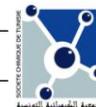
4. Conclusion:

The photocatalytic degradation of RY23 in aqueous solution was studied using TiO2 Degussa P-25 as a semiconductor catalyst. Adsorption plays an essential role in the degradability of the dye. By comparing the rate of disappearance of RY23 (followed by HPLC-DAD) with that of the bleaching of the solution (followed by UV-Vis spectrometry), it was put evidence some of the intermediate products are also colored. This result was confirmed using HPLC-DAD and HPLC-MS analysis. This study confirms that photocatalysis is suitable to the decolorizingcolored aqueous effluents.

References:
[1] H. Zollinger (Ed), color chemistry: Synthesis, Properties and Applications of Organic Dyes and pigments, second revised ed.,*VCH*, **1991**.
[2] J. Weber, V.C. Stickney, *Wat. Res*, **1993**, **27**, 63.
[3] C. Rafols, D. Barcelo, *J. chromatogr A*, **1997, 777**, 177.
[4] A. Houas, H. Lachheb, M. Ksibi, E. Elaloui, C.Guillard, J.M. Hermann, ***Appl.catal. B: Environ***, **2001**, **31**, 145.
[5] I.K. Konstantinou, T.A. Albanis, ***Appl.catal. B: Environ, 2004***, **49**, 1-14.
[6] M. Schiavello (Ed), *Photocatalysis and environment: Trends and Applications*, NATO ASI Series C, vol. 238 Kluwer Academic Published, London, **1987**.
[7] D.F. Ollis, H. Al-Ekabi (Eds), *Photocatalytic Purification and Treatement of Water and Air*, Elsevier, Amsterdam, **1993**.
[8] O. Legrini, E. Oliveros, A. Braun, *chem. Rev*, **1993**, **93**, 671-698.
[9] D. Bahnemann, J. C unningham, M.A. Fox, E. Pelliziti, P. Pichat, N. Serpone, in: G.R. Zepp, D.G. Crosby (Eds.), *Aquatic and Surface photochemistry*, Lewis, Boca Raton, FL, **1994**.
[10] D.M. Blake, *Bibliography of work on the photocatalytic removal of hazardous compounds from water and air*, NREL/TP-430-22197, National Renewable Energy Laboratory, Golden Co., **1997, 1999**.
[11] J.M. Herrmann, *Catal, Today* **1999**, **53**, 115-129.
[12] J.M. Herrmann, in: F Jansen, R.A. van santen (Eds.), Water Treatment by Heterogenous Photocatalysis in Environmental Catalysis, *Catalysis Science Series*, vol. 1, Imperial College Press, London, **1999**, Chapter 9, p. 171-194.
[13] E. Pelizzetti, E. Minero, C. Pramauro, in: H.I Lasa, G. Dogu, A. Ravella (Eds.), *Chemical Reactor Technology for Environmentally Safe Reactors and Products*, Kluwer Academic Publishers, Dordrecht, The Netherlands, **1993**, 77.
[14] P.C Vandevivere, R. Bianchi, W. Verstraete, *J. Chem. Technol. Biotechnol*, **1998**, **72**, 289.
[15] R.W. Matthews, *J. Phys. Chem*., **1987,91**, 3328-3333.
[16] I. Bouzaida, C. Ferronato, J.M. Chovelon, M.E. Rammah, J.M. Herrmann, Heterogeneous photocatalytic degradation of the anthraquinonic dye, Acid Blue 25 (AB25): a kinetic approach, *Journal of Photochemistry and Photobiology A: Chemistry*., **2004**, **168**, 23-30.
[17] C.Bauer, P.Jacques, A.Kalt, Photodegradation of an azo dye induced by visible light incident on the surface of TiO$_2$, *Journal of Photochemistry and Photobiology A : Chemistry*., **2001**, **140**, 87-92.
[18] C.Galindo, P.Jacque, A.Kalt, Photooxidation of the phenylazonaphtol AO20 on TiO$_2$: kinetic and mechanistic investigations, *Chemosphere*., **2001,45**, 997-1005.
[19] C.Galindo, P.Jacque, A.Kalt, Photodegradation of the aminoazobenzene acid orange 52 by three advanced oxidation processes : UV/H$_2$O$_2$, UV/TiO$_2$ and VIS/TiO$_2$. Comparative mechanistic and kinetic investigations, *Journal of Photochemistry and Photobiology A : Chemistry*., **2000**, **130**, 35-47.
[20] K. Tanaka K., K. Padermpole, T. Hisanaga, Photocatalytic degradation of commercial azo dyes, *Water Research*., **2000**, **34**, 327-333.
[21] N. Daneshvar, D. Salari, A.R. Khataee, Photocatalytic degradation of azo dye acid red 14 in water: investigation of the effet of operational parameters, *Journal of Photochemistry and Photobiology A : Chemistry*., **2003**, **157**, 111-116.
[22] C. Hu, Y. Wang, Decolorization and biodegradability of photocatalytic treated azo dyes and wool textile waste water., *Chemosphere*., **1999**, **39**, 2107-2015.
[23] G.A. Epling, C. Lin, Photoassisted bleaching of dyes utilizing TiO$_2$ and visible light, *Chemosphere*., **2002**, **46**, 561-570.
[24] H. Lachheb, E. Puzenat, A. Houas, M. Ksibi, E. Elaloui, C.Guillard, J.M. Herrmann, Photocatalytic degradation of various types of dyes (Alizarin S, Crocein Orange G, Methyl Red, Congo Red, Methylene Blue) in water by UV-irradiated titania, *Applied Catalysis B : Environmental*., **2002**, **39**, 75-90.
[25] E. Vulliet, C. Emmelin, J.M. Chovelon, C. Guillard, J.M. Herrmann, Photocatalytic degradation of sulfonylurea herbicides in aqueous TiO$_2$, *Applied Catalysis B : Environmental*., **2002**, **38**, 127-137.